*J. Iran. Chem. Soc.*, Vol. 7, No. 4, December 2010, pp. 934-945.

JOURNAL OF THE
Iranian
Chemical Society

# Conformational Stabilities, EPR, IR and VCD Studies of Tris(ethylenediamine)nickel(II) Chloride

N. Noorani[a], H. Rahemi[b,*] and S.F. Tayyari[c]
[a]*Payam-Noor University, Urmia, Urmia, Iran*
[b]*Chemistry Department, Urmia University, 57159-165, Iran*
[c]*Chemistry Department, Ferdowsi University of Mashhad, Mashhad, 91775-1435, Iran*

*(Received 11 December 2009, Accepted 18 February 2010)*

Conformational stabilities of the transition metal complex of the $[Ni(en)_3]Cl_2$ was studied using Density Functional Theory (DFT). The deformational potential energy profiles (PEPS), pathways between the different isomeric conformational energies were calculated using B3LYP/6-31G. Relative conformational energies of the Δ(λλλ), Δ(λλδ), Δ(λδδ) and Δ(δδδ) were 0.04, 0.36, 0.17, 0.0 kcal $mol^{-1}$, respectively, which were small compared to the barrier heights for the reversible phase transitions 51.12, 50.48, 49.64 kcal $mol^{-1}$, respectively. The frequency assignment was carried out by fitting Fourier transform infrared (FTIR) spectra and using Gaussian and GaussView computer programs. The theoretical vibrational circular dichroism (VCD) absorption spectra are presented for all conformations in the range of 400-3500 $cm^{-1}$. Calculated electron paramagnetic resonance (EPR) g-tensor parameters of the $[Ni(en)_3]Cl_2$, $g_x = 2.69$, $g_y = g_z = 2.71$, are well compared to the corresponding experimental values and indicate a spherical electronic structure for the Ni atom in this compound.

**Keywords:** Tris(ethylenediamine)nickel(II) chloride, Conformational stabilities, Fourier transform infrared spectra, Vibrational circular dichroism, Electron paramagnetic resonance

## INTRODUCTION

Five-membered ethylenediamine chelate rings have two possible conformations known as δ and λ. When three such chelates form a tris complex, the metal center is chiral and will have two possible enantiomeric configurations known as Δ and Λ. Combining all the structural possibilities results, even for the simple symmetrical chelate ethylene-diamine(en), in a total of eight isomers: Δ(δδδ), Δ(δδλ), Δ(δλλ), Δ(λλλ) and Λ(δδδ), Λ(δδλ), Λ(δλλ), Λ(λλλ). In a non-chiral medium, the discussion can be limited to the first four of these isomers with the realization that all arguments apply equally well to their appropriate mirror images [1-4]. In the Λ configuration, the δ ring conformation is achieved when the carbon-carbon bond is nearly parallel to the threefold axis and the λ ring conformation is assigned where this bond forms an obtuse angle with the C3 axis. Due to the identical conformational stabilities of their mirror image set, the following discussion will be limited to only the first set of four conformers in the above list (Fig. 1).

The transition metal complexes of the general form $M(en)_3^{n+}$ are ideal host lattices for single crystals. Many studies have investigated their electron paramagnetic resonance (EPR), reversible phase transitions, and optical activities for electronic dichroism spectroscopy (ECD) and vibrational dichroism spectroscopy (VCD) [5-9].

*Corresponding author. E-mail: hrahemi@yahoo.com

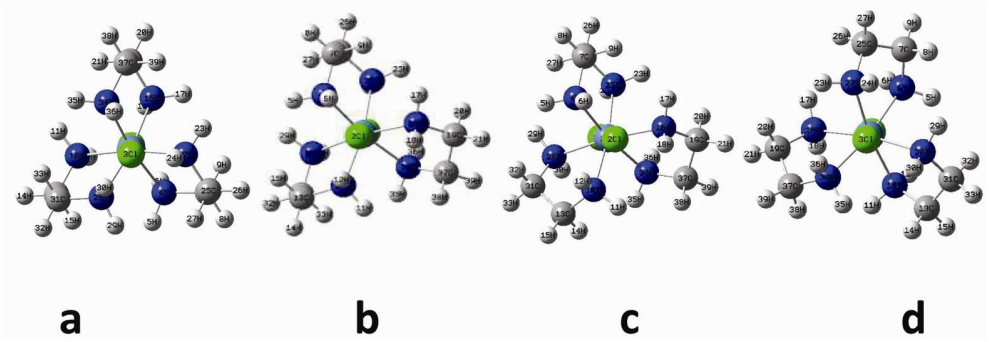


**Fig. 1.** The B3LYP/6-31G optimized structure of the $Ni(en)_3Cl_2$. a) Δ(λλλ), b) Δ(δλλ), c) Δ(δδλ) and d) Δ(δδδ) conformations, displayed view along the $C_3$ symmetry axis.

The tris(ethylenediamine)nickel(II) $[Ni(en)_3]^{2+}$ lattice (where en = ethylenediamine) has already been used as a host to study the electron paramagnetic resonance (EPR) of metal tris$(en)_3$ complex [10,11]. The phase transition of the $[Ni(en)_3]^{2+}$ lattice was first observed in the EPR spectra of the $[Mn(en)_3]^{2+}$ complex, although the overlapping spectra of the many magnetically distinct sites at low temperature precluded a full analysis. Later, it was realized [11] that the $[Ni(en)_3]^{2+}$ complex was a better structural probe of the host, since the absence of nuclear hyperfine interactions greatly simplifies the EPR spectra. Consequently, axially symmetric spin Hamiltonian parameters were found which were interpreted as arising from the fast interconversion of conformers with orthorhombic symmetry. EPR g-tensor parameters of the $[Ni(en)_3]^{2+}$ with two unpaired electrons were also calculated for the electronic structure determination of Ni atom. In this work, we employed computational studies as a complementary technique to aid us to become acquainted with the electronic and geometric structures of the nickel complexes. Specifically, we made some calculations on the relative stability and transition state pathways between various conformational isomers of the coordination compounds. Their VCD and IR absorption spectra are reported for $[Ni(en)_3]Cl_2$.

## THEORETICAL AND COMPUTATIONAL DEVELOPMENTS

The computer program used was the Gaussian 03W [12] and all calculations were made at the DFT level. The underlying theory was the Kohn Sham approach to DFT [13] which uses one particle Schrodinger equation and performs self-consistent field (SCF) procedures. The Vosko, Wilk and Nusair (VWN) [14] formula for local density approximation and for general gradient approximation (GGA), Becke3 (B3) [15] for exchange correction term and Lee-Yang-Parr (LYP) [16] for correlation correction term, all with B3LYP functional and with a reasonable large basis set of 6-31G were used. The g-tensor values were calculated using the DFT/GIAO methods by the B3LYP/6-31G and B3LYP/6-31G** level as implemented in Gaussian 03.

## EXPERIMENTAL

The tris(ethylenediamine) nickel(II) chloride, $[Ni(en)_3]Cl_2$, was prepared by adding excess ethylenediamine to an aqueous solution of nickel chloride. When the product precipitated from solution upon the addition of acetone, it was immediately filtered [17,18] and dried.

KBr tablets of $[Ni(en)_3]Cl_2$ were prepared and the FTIR spectrum in the 400-4000 $cm^{-1}$ region was taken using the FT-IR Thermonicolet, Nexus-670 spectrophotometer.

## RESULTS

### Transition State Pathways

The Z-Matrix of $[Ni(en)_3]^{2+}$ was constructed using five dummy atoms, two along $C_3$ axis and three along $C_2$ axes, for the symmetry adjustments. The B3LYP/6-31G optimizations

of the complexes were done with an acceptable accuracy; the selected bond lengths and bond angles values are given in Table 1. The minor differences can be attributed to the fact that the calculated values have been obtained for the gas phase while the corresponding experimental values are for the solid state [19]. While calculating the conformational pathways, it was found that variations of two dihedral angles, H-N-Ni-X (D2) and H-C-N-H (D5) were required. Other variables were carefully designed to adjust themselves to D2 and D5. Except for D2 and D5, all other bond lengths and bond angles did not change significantly from one conformer to the other one; therefore, mean values were calculated and taken into account in the potential energy profile calculations. Unfortunately, running a grid scan for both angles at the same time was not possible due to the instability of the complex in large deviations from the optimized conformations. Therefore, D2 and D5 were varied step by step (35 separate runs, single point calculation) to calculate conformational pathway energies. The pathway between different conformers of $[Ni(en)_3]^{2+}$ is presented in Fig. 2. Conformational energies and reversible phase transition barrier heights are listed in Table 2. The calculated order of the stability of the $[Ni(en)_3]^{2+}$ isomers are $\Delta(\lambda\lambda\lambda) > \Delta(\lambda\lambda\delta) > \Delta(\lambda\delta\delta) > \Delta(\delta\delta\delta)$ within a fraction of 1 kcal $mol^{-1}$ jump between the corresponding conformations. Therefore, the appearance of various isomers in different crystalline structures, having high reversible phase transition barriers of about 41.50 kcal $mol^{-1}$, were rather accidental.

Similarly, the same calculations were made for $[Ni(en)_3]Cl_2$ in free space. The results are given in Table 2 and Fig. 2. By comparing the calculated results for $[Ni(en)_3]^{2+}$ and $[Ni(en)_3]Cl_2$ it was concluded that the inclusion of the chlorine atoms elevated the barrier height for about 9 kcal $mol^{-1}$. The

**Table 1.** Optimized Bond Lengths (Å) and Bond Angles (°) of the Tris(ethylenediamin)nickel(II)

| | B3LYP/6-31G** | | | | |
|---|---|---|---|---|---|
| Geometry | Δ(λλλ) | Δ(λλδ) | Δ(λδδ) | Δ(δδδ) | Expt. [16] |
| Bond length (Å) | | | | | |
| Ni-Cl | 3.90 | 3.87 | 3.82 | 3.78 | |
| Ni-N37 | 2.18 | 2.17 | 2.18 | 2.18 | 2.18(1) |
| Ni-N31 | 2.18 | 2.17 | 2.18 | 2.18 | 2.17(1) |
| Ni-N25 | 2.18 | 2.17 | 2.18 | 2.18 | 2.16(2) |
| N-C (all) | 1.48 | 1.48 | 1.48 | 1.48 | 1.48(3) |
| CN-CN(all) | 1.51 | 1.52 | 1.52 | 1.53 | 1.47(4) |
| Bond angle (º) | | | | | |
| N13-Ni-N25 | 167.95 | 168.66 | 170.62 | 172.62 | 170.5(0.6) |
| N7-Ni-N37 | 167.95 | 170.17 | 170.62 | 172.62 | 170.5(0.6) |
| N19-Ni-N31 | 167.95 | 170.17 | 172.13 | 172.62 | 170.5(0.6) |
| N13-Ni-N25 | 79.33 | 80.53 | 79.33 | 79.33 | 79.8(0.6) |
| N7-Ni-N37 | 79.33 | 80.53 | 79.56 | 79.33 | 79.8(0.6) |
| N19-Ni-N31 | 79.33 | 80.24 | 79.56 | 79.33 | 79.8(0.6) |
| Ni-N-C | 108.32 | 108.32 | 108.32 | 108.32 | 108.1(1.5) |
| N-C-C | 109.72 | 110.19 | 109.72 | 109.47 | 108.9(2.4) |
| N-C-C | 109.72 | 110.19 | 110.02 | 109.47 | 108.9(2.4) |
| N-C-C | 109.72 | 110.96 | 110.02 | 109.47 | 109.9(1.9) |

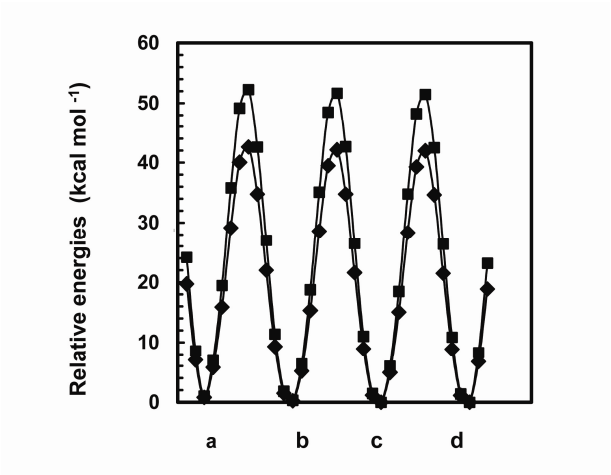


**Fig. 2.** Relative conformational path ways between isomers: (◆) $Ni(en)_3Cl_2$ and (■) $Ni(en)_3^{2+}$.

**Table 2.** Relative Conformational Energies and Barriers Heights of $[Ni(en)_3]Cl_2$ and $Ni(en)_3^{2+}$ Using Optimized Geometry Variables

| Conformer | $Ni(en)_3^{2+}$, solid | $[Ni(en)_3]Cl_2$ |
|---|---|---|
| Δ(λλλ) | 0.63 | 0.04 |
| barrier 1 | 41.48 | 51.12 |
| Δ(λλδ) | 0.17 | 0.36 |
| barrier 2 | 41.02 | 50.48 |
| Δ(λδδ) | 0.01 | 0.17 |
| barrier 3 | 40.97 | 49.64 |
| Δ(δδδ) | 0.00 | 0.00 |

most stable conformer within a fraction of kcal $mol^{-1}$ was Δ(δδδ).

## IR and Vibrational Circular Dichroism Spectra

The FTIR spectrum of the complex in 400-4000 $cm^{-1}$ region is shown in Fig. 3. Calculation of the vibrational frequency spectrum of a nonlinear molecule containing N centers led to 3N-6 true vibrational normal modes. As these are usually not localized motions of a small part of the molecule, assignment of the individual modes can, particularly in larger systems, be somewhat difficult. Several strategies can be used to facilitate the assignment systems: The vibrational band assignments could be set by: (1) constructing the IR absorption spectrum of the $[Ni(en)_3]Cl_2$ using Lorenzian line shape fitted to the experimental spectrum, (2) Animating Gaussian output vibrational bands using Gaussview and Hyperchem (Fig. 4 and Table 3).

The optical activity of dissymmetric molecules is explained when a plane polarized radiation passes through an active medium. The plane of the emergent plane polarized radiation rotates by an angle. The plane polarized beam can be considered as a superposition of two oppositely rotating circularly polarized components. The absorbance coefficient is defined [20] as $\Delta\varepsilon = \varepsilon_L - \varepsilon_R$ and the line shape is nearly Gaussian. The absorbance coefficient of the VCD is given by

$$\Delta\varepsilon = \frac{2\sqrt{\ln 2}R\bar{\nu}}{2.296\times10^{-39}\sqrt{\pi}\Gamma_{1/2}}\exp\left[4\ln(2)\left(\frac{\bar{\nu}-\bar{\nu}_0}{\Gamma_{1/2}}\right)^2\right] \quad (1)$$

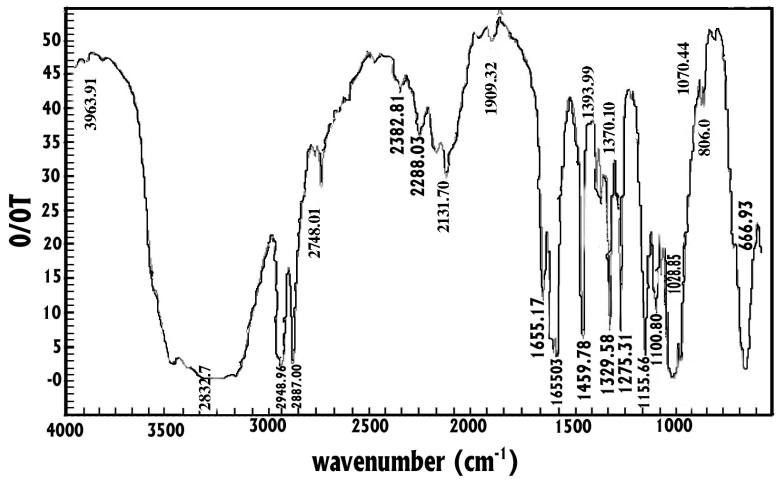


**Fig. 3.** The FTIR transmittance spectrum of the solid $Ni(en)_3Cl_2$.

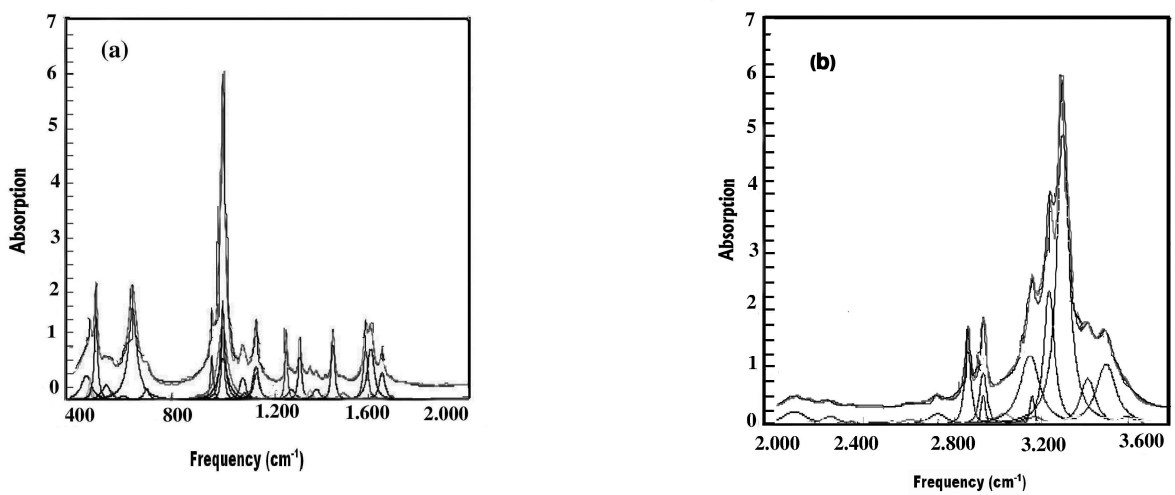


**Fig. 4.** The $Ni(en)_3Cl_2$ FTIR spectra is decomposed theoretically for frequency assignments (a) between 400 $cm^{-1}$-2000 $cm^{-1}$, (b) between 2000 $cm^{-1}$-3600 $cm^{-1}$.

**Table 3.** Frequency Assignment of the Ni Complex Be = Bending, Ro = Rocking, Tw = Twisting, Sc = Scissoring, Str = Stretching, Wa = Wagging and E, A, B, $A_1$, $A_2$ are Irreducible Representations of the Corresponding $D_3$ and $C_2$ Symmetry Point Groups. Scalling Factor of 0.97 are Used

| | | B3LYP/6-31G Tris(ethylenediamin)Nickelchloride/$Ni(en)_3Cl_2$ | | | | B3LYP/6-31G Tris(ethylenediamin) Nickel (II)/$Ni(en)_3^{2+}$ | | | | Expt. |
|---|---|---|---|---|---|---|---|---|---|---|
| No. | Assignment | Δ(λλλ) | Δ(λλδ) | Δ(λδδ) | Δ(δδδ) | Δ(λλλ) | Δ(λλδ) | Δ(λδδ) | Δ(δδδ) | |
| 1 | $NiCl_2$, Be | 63.5 | 58.1 | 55.4 | 61.1 | | | | | |
| 2 | $NiCl_2$, Be | 63.6 | 67. | 56.7 | 61.1 | | | | | |
| 3 | $NiCl_2$, Be | 86.2 | 71.0 | 66.2 | 65.7 | | | | | |
| 4 | $NiCl_2$, Be | 86.2 | 89.8 | 66.5 | 65.7 | | | | | |
| 5 | $NiCl_2$, Str | 98.4 | 100.1 | 99.6 | 92.9 | | | | | |
| 6 | $NiCl_2$, Str. | 110.2 | 105.3 | 103.8 | 104.8 | | | | | |
| 7 | NiNC, Be | 111.5 | 110.1 | 106.1 | 104.8 | 48.7 | 64.8 | 65.6 | 62.9 | |
| 8 | NiNC, Be | 111.5 | 111.9 | 111.5 | 112.1 | 48.7 | 67.8 | 69.6 | 62.9 | |
| 9 | $NiN_2$, Tw | 148.6 | 138.9 | 132.2 | 134.8 | 56.9 | 79.9 | 84.7 | 78.5 | |
| 10 | $NiN_2$, Tw | 148.6 | 148.8 | 144.2 | 134.8 | 89.2 | 95.1 | 88.1 | 90.7 | |
| 11 | NiNC, Be | 158.6 | 153.5 | 151.9 | 149.8 | 89.2 | 98.3 | 91.9 | 90.7 | |
| 12 | $NiN_2$, Tw | 162.9 | 163.1 | 162.5 | 159.1 | 102.4 | 109.8 | 105.6 | 113.1 | |
| 13 | $NiN_2$, Wa | 209.0 | 191.0 | 180.2 | 179.4 | 153.8 | 157.7 | 156.6 | 157.3 | |
| 14 | $NiN_2$, Wa | 209.0 | 205.8 | 192.5 | 179.4 | 161.5 | 163.4 | 157.0 | 157.3 | |
| 15 | $NiN_2$, Wa | 213.1 | 218.7 | 220.2 | 206.7 | 161.5 | 168.8 | 160.2 | 167.4 | |
| 16 | $NiN_2$, Str | 224.5 | 219.8 | 220.7 | 225.3 | 184.9 | 190.1 | 190. 1 | 193.1 | |
| 17 | $NiN_2$, Str | 224.5 | 225.9 | 223.9 | 226.5 | 205.4 | 204.4 | 204.9 | 211.6 | |
| 18 | $NiN_2$, Str | 231.2 | 227.4 | 225.4 | 226.5 | 205.4 | 209.8 | 207.4 | 211.6 | |
| 19 | $NiN_2$, Str | 272.3 | 263.2 | 253.4 | 251.5 | 259.2 | 259.6 | 253.8 | 251.5 | |
| 20 | $NiN_2$, Str | 272.3 | 275.8 | 259.6 | 251.5 | 259.2 | 260.2 | 259.5 | 251.5 | |

**Table 3.** Continued

| | | | | | | | | | | |
|---|---|---|---|---|---|---|---|---|---|---|
| 21 | $NiN_2$, Str | 291.6 | 285.3 | 285.0 | 262.2 | 267.0 | 270.2 | 274.9 | 272.8 | |
| 22 | NCC, Be | 291.6 | 293.5 | 287.2 | 293.2 | 267.0 | 276.7 | 277.6 | 272.8 | |
| 23 | NCC, Be | 307.6 | 302.2 | 300.1 | 293.2 | 278.0 | 278.6 | 278.5 | 273.7 | |
| 24 | NCC, Be | 308.0 | 306.6 | 308.8 | 308.2 | 284.6 | 287.3 | 283.9 | 286.8 | |
| 25 | $NiN_2$, Sc | 393.7 | 393.9 | 400.1 | 403.7 | 366.4 | 367.5 | 365.4 | 365.4 | |
| 26 | $NiN_2$, Sc | 393.7 | 398.8 | 403.0 | 403.7 | 366.4 | 369.6 | 368.3 | 365.4 | |
| 27 | $NiN_2$, Sc | 418.7 | 420.7 | 425.3 | 427.6 | 394.7 | 394.4 | 396.8 | 400.6 | |
| 28 | $CH_2$, $NH_2$, Ro | 497.6 | 503.2 | 513.4 | 521.9 | 468.6 | 476.7 | 485.3 | 493.8 | 520 |
| 29 | $CH_2$, $NH_2$, Ro | 529.3 | 523.4 | 521.6 | 521.9 | 508.8 | 495.5 | 488.3 | 493.8 | 530 |
| 30 | $CH_2$, $NH_2$, Ro | 529.3 | 530.7 | 529.1 | 532.9 | 508.8 | 512.5 | 507.7 | 504.4 | 530 |
| 31 | $CH_2$, $NH_2$, Ro | 615.3 | 601.6 | 600.5 | 581.5 | 531.1 | 548.3 | 558.4 | 575.7 | 590 |
| 32 | $CH_2$, $NH_2$, Ro | 615.3 | 621.2 | 607.2 | 606.2 | 531.1 | 552.9 | 568.5 | 587.7 | 608 |
| 33 | $CH_2$, $NH_2$, Ro | 692.5 | 650.4 | 615.8 | 606.2 | 629.2 | 621.5 | 604.2 | 588.0 | 608 |
| 34 | $NH_2$,Tw+$CH_2$,Ro | 704.2 | 688.2 | 664.7 | 630.3 | 640.4 | 630.5 | 605.7 | 588.0 | |
| 35 | $NH_2$,Tw+$CH_2$,Ro | 724.6 | 722.0 | 710.4 | 705.3 | 640.4 | 645.3 | 661.8 | 687.5 | 713 |
| 36 | $NH_2$,Tw+$CH_2$,Ro | 724.6 | 732.7 | 730.6 | 705.3 | 657.9 | 678.2 | 686.0 | 687.5 | 759 |
| 37 | NC+CC, Str | 859.7 | 857.6 | 857.8 | 857.5 | 847.6 | 844.5 | 843.1 | 843.0 | 859 |
| 38 | NC+CC, Str | 859.7 | 859.2 | 858.7 | 857.5 | 847.6 | 846.4 | 847.1 | 843.0 | 859 |
| 39 | NC+CC, Str | 863.4 | 862.8 | 860.8 | 860.0 | 851.2 | 850.2 | 850.3 | 849.7 | |
| 40 | NC+CC, Str | 866.3 | 862.8 | 863.3 | 860.0 | 851.2 | 851.1 | 850.9 | 849.7 | 860 |
| 41 | NC+CC, Str | 866.3 | 864.2 | 864.5 | 861.4 | 851.8 | 870.1 | 852.5 | 852.1 | 860 |
| 42 | NC+CC, Str | 875.7 | 873.3 | 931.9 | 870.7 | 853.4 | 856.2 | 858.6 | 859.4 | 900 |
| 43 | $CH_2$,Ro+$NH_2$,Tw | 961.5 | 956.4 | 953.9 | 953.3 | 955.5 | 957.3 | 960.9 | 959.6 | 958 |
| 44 | $CH_2$,Ro+$NH_2$,Tw | 961.5 | 962.5 | 959.1 | 953.3 | 955.5 | 960.6 | 961.4 | 959.6 | 958 |
| 45 | $CH_2$,Ro+$NH_2$,Tw | 969.1 | 967.9 | 968.4 | 963.1 | 964.4 | 965.1 | 966.1 | 964.1 | |
| 46 | NC+CC, Str | 1024.5 | 1023.3 | 1022.8 | 1022.8 | 996.8 | 996.6 | 996.9 | 996.21 | 1022 |
| 47 | NC+CC, Str | 1024.5 | 1023.8 | 1023.3 | 1022.8 | 996.8 | 997.0 | 997.2 | 996.6 | 1022 |
| 48 | NC+CC, Str | 1025.3 | 1024.6 | 1024.9 | 1024.3 | 997.8 | 997.8 | 997.4 | 996.6 | 1025 |
| 49 | $CH_2$,Ro+$NH_2$,Tw | 1029.8 | 1028.2 | 1027.4 | 1027.8 | 1008.1 | 1008.2 | 1009.7 | 1012.2 | 1029 |
| 50 | NC+CC, Str | 1029.8 | 1029.3 | 1029.6 | 1027.8 | 1008.0 | 1009.9 | 1010.0 | 1012.2 | 1029 |
| 51 | NC+CC, Str | 1045.5 | 1046.1 | 1048.9 | 1052.7 | 1025.3 | 1025.3 | 1025.9 | 1028.8 | |
| 52 | HCC + HNC, Be | 1075.5 | 1074.5 | 1072.2 | 1070.8 | 1075.4 | 1080.2 | 1079.7 | 1079.3 | 1075 |
| 53 | HCC + HNC, Be | 1077.8 | 1079.6 | 1077.3 | 1070.8 | 1083.8 | 1083.5 | 1085.2 | 1079.3 | 1078 |
| 54 | HCC + HNC, Be | 1077.8 | 1082.8 | 1087.8 | 1096.9 | 1083. 8 | 1086.2 | 1090.0 | 1129.2 | 1100 |
| 55 | $NH_2$, Wa | 1143.2 | 1134.8 | 1128.8 | 1132.1 | 1130.8 | 1131.0 | 1129.7 | 1133.1 | 1132 |
| 56 | $NH_2$, Wa | 1143.2 | 1135.6 | 1132.9 | 1132.1 | 1130.8 | 1131.2 | 1132.7 | 1133.1 | 1132 |
| 57 | $NH_2$, Wa | 1157.1 | 1147.5 | 1140.8 | 1135.4 | 1144.4 | 1143.4 | 1140.8 | 1149. 1 | 1135 |
| 58 | $NH_2$, Wa | 11571 | 1158.5 | 1145.4 | 1135.4 | 1144.4 | 1147.9 | 1148.8 | 1149. 1 | 1136 |
| 59 | $NH_2$, Wa | 1169.7 | 1168.0 | 1164.6 | 1156.9 | 1145.6 | 1148.1 | 1151.0 | 1150.8 | |
| 60 | $NH_2$, Wa | 1201.5 | 1195.5 | 1186.3 | 1169.3 | 1168.2 | 1168.1 | 1167.7 | 1173.1 | 1170 |
| 61 | HCC+ HNC, Be | 1275.9 | 1264.6 | 1259.7 | 1258.3 | 1282.2 | 1282.4 | 1283.1 | 1283.7 | 1258 |
| 62 | HCC+ HNC, Be | 1275.9 | 1275.2 | 1266.5 | 1258.3 | 1282.2 | 1283.5 | 1283.8 | 1283.7 | 1258 |
| 63 | HCC+ HNC, Be | 1281.8 | 1281.5 | 1279.3 | 1274.2 | 1285.9 | 1287.9 | 1288.7 | 1288.5 | |
| 64 | $CH_2$ +$NH_2$, Tw | 1299.2 | 1289.7 | 1286.8 | 1285.6 | 1297.0 | 1297.1 | 1297.7 | 1297.8 | 1285 |
| 65 | $CH_2$ +$NH_2$, Tw | 1299.2 | 1299.8 | 1289.8 | 1285.6 | 1297.0 | 1298.9 | 1298.4 | 1297.8 | 1285 |

**Table 3.** Continued

| | | | | | | | | | | |
|---|---|---|---|---|---|---|---|---|---|---|
| 66 | $CH_2$ +$NH_2$, Tw | 1306.2 | 1304.6 | 1303.9 | 1290.3 | 1300.0 | 1300.6 | 1302.2 | 1302.9 | |
| 67 | $CH_2$ +$NH_2$, Tw | 1339.2 | 1323.1 | 1318.9 | 1317.8 | 1335.2 | 1336.1 | 1336.4 | 1338.1 | 1318 |
| 68 | $CH_2$ +$NH_2$, Tw | 1339.2 | 1339.2 | 1324.2 | 1317.8 | 1335.2 | 1336.5 | 1337.6 | 1338.1 | 1318 |
| 69 | $CH_2$ +$NH_2$, Tw | 1344.1 | 1343.1 | 1342.1 | 1326.3 | 1336.6 | 1339.4 | 1340.2 | 1340.2 | 1328 |
| 70 | $CH_2$, Wa | 1389.7 | 1388.0 | 1387.7 | 1391.5 | 1398.4 | 1398.4 | 1398.6 | 1398.4 | 1390 |
| 71 | $CH_2$, Wa | 1389.7 | 1389.9 | 1391.2 | 1391.5 | 1398.4 | 1398.6 | 1399.7 | 1398.4 | 1390 |
| 72 | $CH_2$, Wa | 1393.4 | 1392.5 | 1393.2 | 1393.4 | 1398.4 | 1399.5 | 1401.2 | 1401.9 | |
| 73 | $CH_2$, Wa | 1393.6 | 1393.0 | 1393.8 | 1393.4 | 1408.8 | 1408.4 | 1407.3 | 1407.8 | 1393 |
| 74 | $CH_2$, Wa | 1393.6 | 1395.9 | 1396.0 | 1397.1 | 1408.8 | 1408.4 | 1409.1 | 1407.8 | 1400 |
| 75 | $CH_2$, Wa | 1394.0 | 1396.1 | 1396.9 | 1397.2 | 1409.9 | 1409.7 | 1409.7 | 1410.7 | 1401 |
| 76 | $CH_2$, Sc | 1498.1 | 1497.2 | 1500.0 | 1500.1 | 1499.2 | 1499.2 | 1499.6 | 1498.1 | |
| 77 | $CH_2$, Sc | 1498.7 | 1497.6 | 1500.6 | 1500.1 | 1499.6 | 1499.3 | 1499.9 | 1498.2 | 1498.7 |
| 78 | $CH_2$, Sc | 1498.7 | 1500.1 | 1501.4 | 1500.8 | 1499.6 | 1501.7 | 1503.2 | 1498.2 | 1500 |
| 79 | $CH_2$, Sc | 1499.7 | 1500.7 | 1501.5 | 1501.5 | 1502.3 | 1503.1 | 1504.9 | 1501.2 | 1501 |
| 80 | $CH_2$, Sc | 1500.7 | 1500.9 | 1502.5 | 1501.5 | 1503.4 | 1503.7 | 1504.9 | 1501.2 | 1501 |
| 81 | $CH_2$, Sc | 1500.7 | 1501.4 | 1503.6 | 1501.5 | 1503.4 | 1504.5 | 1506.2 | 1501.6 | 1511 |
| 82 | $NH_2$, Sc | 1666.8 | 1660.7 | 1657.9 | 1662.1 | 1653.4 | 1653.8 | 1656.8 | 1665.1 | 1665 |
| 83 | $NH_2$, Sc | 1676.2 | 1672.9 | 1670.3 | 1666.1 | 1664.0 | 1667.1 | 1669.1 | 1671.4 | |
| 84 | $NH_2$, Sc | 1690.2 | 1682.4 | 1671.8 | 1666.1 | 1670.1 | 1671.3 | 1672.4 | 1671.4 | 1668 |
| 85 | $NH_2$, Sc | 1690.2 | 1684.4 | 1673.2 | 1677.1 | 1670.1 | 1672.1 | 1673.5 | 1677.2 | 1677 |
| 86 | $NH_2$, Sc | 1695.9 | 1692.7 | 1690.3 | 1677.1 | 1677.1 | 1680.3 | 1682.8 | 1679.8 | 1677 |
| 87 | $NH_2$, Sc | 1695.9 | 1697.1 | 1690.9 | 1678.2 | 1677.1 | 1684.2 | 1684.0 | 1679.8 | 1678 |
| 88 | $CH_2$, Sym Str | 2947.6 | 2946.0 | 2945.2 | 2944.3 | 2985.8 | 2983.7 | 2983.9 | 2984.5 | 2975 |
| 89 | $CH_2$, Sym Str | 2947.7 | 2947.5 | 2945.4 | 2944.3 | 2985.9 | 2984.7 | 2984.0 | 2984.5 | 2975 |
| 90 | $CH_2$, Sym Str | 2947.7 | 2947.6 | 2946.3 | 2944.6 | 2985.9 | 2986.1 | 2985.2 | 2984.5 | 2985 |
| 91 | $CH_2$, Sym Str | 2959.5 | 2955.4 | 2954.5 | 2953.9 | 2985.9 | 2986.2 | 2985.3 | 2984.8 | 2985 |
| 92 | $CH_2$, Sym Str | 2959.5 | 2959.3 | 2954.9 | 2953.9 | 2986.1 | 2986.3 | 2986.0 | 2984.8 | 2988 |
| 93 | $CH_2$, Sym Str | 2960.4 | 2959.9 | 2957.9 | 2954.7 | 2986.1 | 2986.4 | 2986.1 | 2985.1 | |
| 94 | $CH_2$, Asym Str | 2994.7 | 2986.3 | 2984.6 | 2983.1 | 30290 | 3027.8 | 3027.4 | 3027.1 | 2998 |
| 95 | $CH_2$, Asym Str | 2994.7 | 2993.7 | 2984.8 | 2983.1 | 3029.0 | 3028.8 | 3027.5 | 3027.1 | 2998 |
| 96 | $CH_2$, Asym Str | 2994.9 | 2993.8 | 2990.2 | 2983.5 | 3029.2 | 3028.9 | 3028.3 | 3027.2 | |
| 97 | $CH_2$, Asym Str | 3014.3 | 3005.9 | 3004.3 | 3003.4 | 3040.5 | 3038.6 | 3038.7 | 3038.6 | 3044 |
| 98 | $CH_2$, Asym Str | 3014.5 | 3013.5 | 3004.4 | 3003.4 | 3040.5 | 3040.5 | 3038.7 | 3038.6 | 3045 |
| 99 | $CH_2$, Asym Str | 3014.5 | 3013.6 | 3009.6 | 3003.6 | 3040.5 | 3040.5 | 3039.9 | 3038.6 | 3005 |
| 100 | $NH_2$, Sym Str | 3109.2 | 3085.1 | 3083.2 | 3216.5 | 3352.3 | 3352.0 | 3350.7 | 3352 | 3217 |
| 101 | $NH_2$, Sym Str | 3109.2 | 3091.0 | 3089.7 | 3216.5 | 3352.3 | 3352.4 | 3350.8 | 3352 | 3219 |
| 102 | $NH_2$, Sym Str | 3115.2 | 3124.1 | 3235.1 | 3219.2 | 3352.7 | 3353.3 | 3351.6 | 3352.0 | 3219 |
| 103 | $NH_2$, Sym Str | 3115.2 | 3130.0 | 3237.3 | 3219.2 | 3352.7 | 3353.5 | 3351.8 | 3352.1 | 3221 |
| 104 | $NH_2$, Sym Str | 3164.4 | 3257.2 | 3248.3 | 3236.1 | 3353.1 | 3353.6 | 3352.1 | 3352.2 | |
| 105 | $NH_2$, Sym Str | 3170.3 | 3259.2 | 3250.6 | 3238.4 | 3354.0 | 3353.8 | 3352.3 | 3351.3 | 3350 |
| 106 | $NH_2$, Asym Str | 3409.8 | 3409.4 | 3409.1 | 3431.3 | 3428.7 | 3428.9 | 3427.6 | 3430.1 | 3429 |
| 107 | $NH_2$, Asym Str | 3409.8 | 3409.8 | 3409.5 | 3431.3 | 3428.7 | 3429.4 | 3427.7 | 3430.3 | 3429 |
| 108 | $NH_2$, Asym Str | 3410.4 | 3411.2 | 3431.1 | 3431.8 | 3429.6 | 3430.0 | 3429.3 | 3430.6 | 3430 |
| 109 | $NH_2$, Asym Str | 3410.4 | 3413.2 | 3431.3 | 3431.8 | 3429.6 | 3430.4 | 3429.3 | 3430.6 | 3430 |
| 110 | $NH_2$, Asym Str | 3410.5 | 3434.8 | 3432.1 | 3431.9 | 3430.7 | 3431.4 | 3430.0 | 3430.9 | |
| 111 | $NH_2$, Asym Str | 3410.7 | 3435.2 | 3432.4 | 3432.5 | 3431.4 | 3431.5 | 3430.3 | 3430.9 | 3431.5 |

where R is the rotational strength and $\Gamma_{1/2}$ is the full width at the half height. Through reading the rotational constant from Gaussian output, and using the constant full line width of 20 $cm^{-1}$ similar to the IR absorbance spectra, VCD absorption spectra were constructed (Figs. 5-7).

When the complex, $[Ni(en)_3]Cl_2$, was due to the flipping of the C-C backbone in one of the ethylenediamine ligands from δ to λ form, the resulting Δ(λλλ) to Δ(δλλ) conformational change reduced the symmetry to $C_2$. This type of conformational change, even if it did not move the N atom but influenced the electronic properties as a change in the Ni-N-C angle, can influence the direction of the bonding N orbitals. Small amounts of " bent bonding " were required in the interpretation [21] of the circular dichroism of the $[Ni(en)_3]Cl_2$.

The vibrations appeared in groups of three or six, depending on ring deformations or functional groups like $CH_2$ or $NH_2$ stretching or bending activities. The major frequency shifts among different conformations were in the area 400-700 $cm^{-1}$, where the $CH_2$ + $NH_2$ rock, $CH_2$ twist + $NH_2$ rock occur. And in the area 1600-1700 $cm^{-1}$, $NH_2$ and $CH_2$ scissorings occur. In the bending area, almost all of the H atoms were moving; therefore, assignments were rather uncertain. However, the most dominant and active modes were assigned. Unlike functional frequencies, the skeleton frequencies for different conformers, as expected, were shifted and some appeared with different intensities.

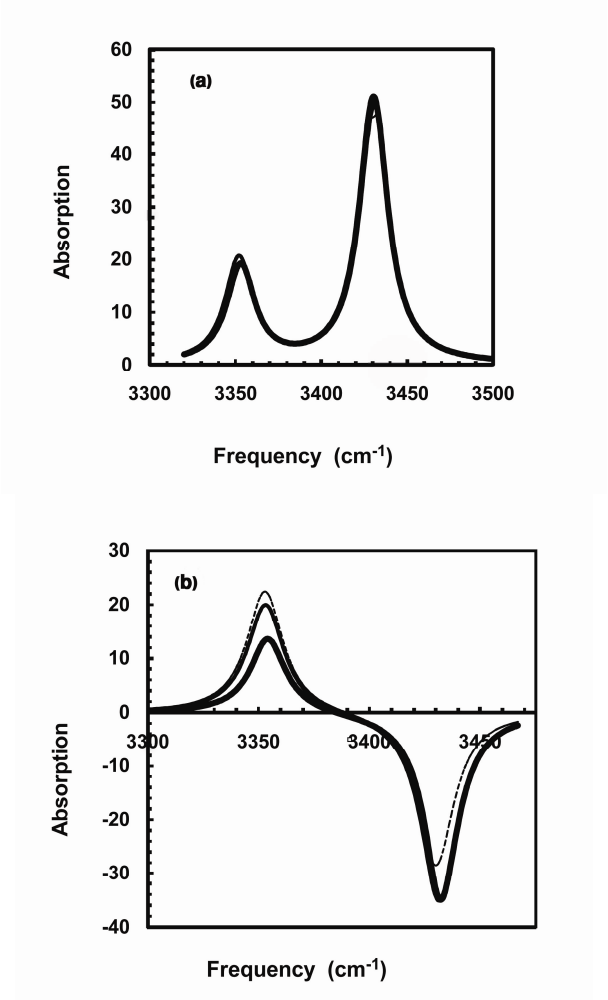


**Fig. 5.** (a) IR spectra (b) VCD spectra of $NH_2$ symmetry and asymmetry stretching modes. Series ---a Δ(λλλ), --- b Δ(δλλ), ---c Δ(δδλ) and …d Δ(δδδ) conformations.

## DISCUSSIONS

The VCD measurements were more analytical than the corresponding IR experiments due to the experimental settings Eq. (2), where alien errors accumulated in the IR, but cancelled out in the VCD.

$$\text{IR;} \quad \Delta\varepsilon = \varepsilon_L + \varepsilon_R \qquad (2)$$

$$\text{VCD;} \quad \Delta\varepsilon = \varepsilon_L - \varepsilon_R$$

In the geometry optimization, both dihedral angles H-N-Ni-X and H-C-N-H had the major roles from one conformation to the other. These two angles could equally be considered to be the H-N-C and H-C-N out of plane bending modes, and it was expected that the combination of $CH_2$ and $NH_2$ bending to be affected by the conformational change. IR vibrational modes for all four conformations except $NH_2$ wagging at 1133 and 1173 $cm^{-1}$, HCC + HNC bending at 1079 $cm^{-1}$ and the 400-700 $cm^{-1}$ area appeared in the same frequencies and intensities, but VCD band polarization changed giving a detailed structural modes, easy for conformational distinction.

Different areas of the $[Ni(en)_3]^{2+}$ complex were magnified to investigate the behavior of the involved vibrational modes with respect to the right and left polarizations. $NH_2$ asymmetry stretching at 3430 $cm^{-1}$ for the conformations Δ(λλλ), Δ(λλδ),

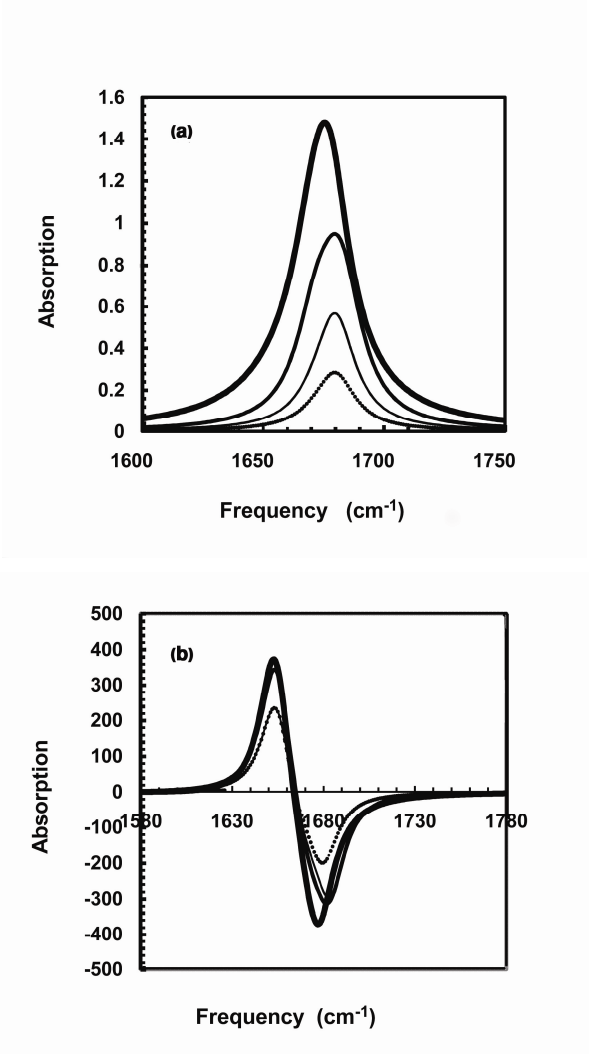


**Fig. 6.** (a) IR spectra (b) VCD spectra of $NH_2$ scissoring modes. Series ---a Δ(λλλ), ---b Δ(δλλ), ---c Δ(ββλ) and …d Δ(δδδ) conformations.

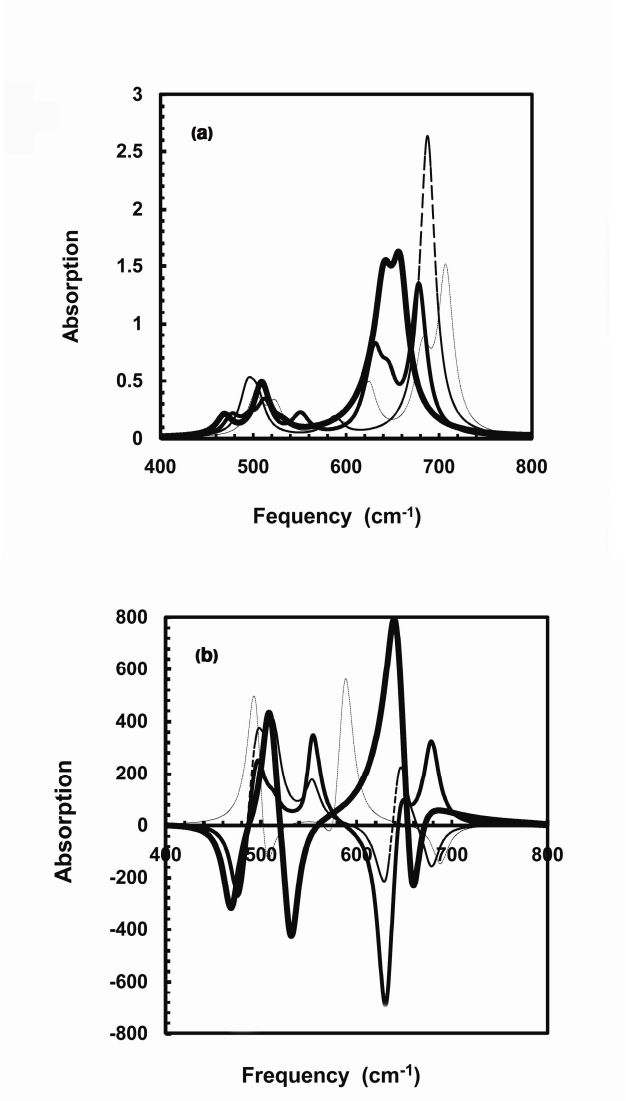


**Fig. 7.** (a) IR spectra (b) VCD spectra of Ni-N skeleton modes. Series ---a Δ(λλλ), ---b Δ(δλλ), ---c Δ(ββλ) and …d Δ(δδδ) conformations.

Δ(λδδ) to Δ(δδδ) lost right polarization intensities by about ¼ and gained left activity for each step of deformational change. $NH_2$ symmetry stretching at 3352 $cm^{-1}$ for all conformations appeared at the same frequency and intensity for both IR and VCD, suggesting invariance according to the polarized light (Fig. 5).

$CH_2$ asymmetry stretching at 3028 and 3038 $cm^{-1}$ for Δ(λλλ) conformation was right polarized whereas for $CH_2$ symmetry stretching at 2985 $cm^{-1}$ was left polarized. The Δ(λλδ) structure lost about ½ of the corresponding intensities and gained opposite polarization, and the situation continued for the Δ(λδδ) complex and ended at the reverse for the Δ(δδδ) conformation.

Unlike Fig. 5, there was no frequency shift from one isomer to the other one for the $NH_2$ scissoring bands at 1665 $cm^{-1}$ and 1679 $cm^{-1}$. These two bands were in fact combination of six (1665, 1671, 1671, 1677, 1679 and 1679 $cm^{-1}$) transitions. The intensity of the outer bands decreased and the inner bands gained intensity in each conformational change from Δ(λλλ) to Δ(δδδ) complexes and finally only one strong

band appeared at 1666 $cm^{-1}$ (Fig. 6). While in VCD, the band at 1665 $cm^{-1}$ from left polarization died out in a step of ¼, the band at 1672 $cm^{-1}$ from right polarization died in a slower rate. The same behavior as for $CH_2$ stretching was seen for $CH_2$ scissoring at 1501 $cm^{-1}$.

$NH_2$ wagging at 1133 $cm^{-1}$ shifted to higher frequency by a step of about 3 $cm^{-1}$ from Δ(λλλ) to Δ(δδδ) and HCC + HNC bending at 1079 $cm^{-1}$ shifted to lower frequency. Shifting frequency and polarization gave a complex behavior to the VCD spectra. $CH_2$ wagging at 1399 $cm^{-1}$ had trends similar to the conformation changes (Table 3).

$NH_2$+$CH_2$ twisting 1297 and at 1340 $cm^{-1}$, and C-C+C-N stretches, area 843-1028 $cm^{-1}$, the frequency shift was about 1 $cm^{-1}$ for each step of the conformational change, but for the example optical activity of the band at 1297 $cm^{-1}$ of Δ(λλλ) conformer from right polarization lost about ½ intensity to Δ(λλδ) conformer and changed to the left polarization for Δ(λδδ) and Δ(δδδ) (Table 3).

The area, 175-400 $cm^{-1}$ Ni-N stretch, where optical activity did not change, intensity changed from Δ(λλλ) to Δ(δδδ). The skeleton area, 400-675 $cm^{-1}$ (Fig. 7), due to the appearance of many transitions which occur in a small area, intensity changes, shifting and overlapping frequencies, provided interesting features.

The combination of the $NH_2$ and $CH_2$ twisting and rocking modes, occurred in the 400-700 $cm^{-1}$ region where one expects some frequency shifts among different isomers. The variation of the $\nu_{22}$ and $\nu_{29}$ with the conformation change for Δ(δδδ), Δ(δδλ), Δ(δλλ) and Δ(λλλ) are plotted in Fig. 8.

The calculated EPR g values from g-tensor parameters (Table 4) of the $[Ni(en)_3]^{2+}$ show that 6-31G** basis sets give better trends compared with the experimental values. Assuming that polarized orbital was a better choice in EPR calculations for Δ(λλλ) conformer, we have $g_\perp = ( g_x + g_y)/2$ = 2.70 and $g_\parallel = g_z$ = 2.71, which indicate that the nature of chilate bonds in the complex causes Ni to resume its almost spherical symmetry. The calculated g values for Δ(δδδ) conformer of $[Ni(en)_3]^{2+}$, $[Ni(en)_3]Cl_2$ are $g_x$ = 2.69, $g_y = g_z$ 2.71, and the experimental values of the $[Ni(en)_3](NO_3)_2$ are $g_x$ = 2.68, $g_y = g_z$ = 2.71 within the calculated and experimental accuracy are the same, therefore, anion role in EPR calculation of this type of complex is negligibly small.

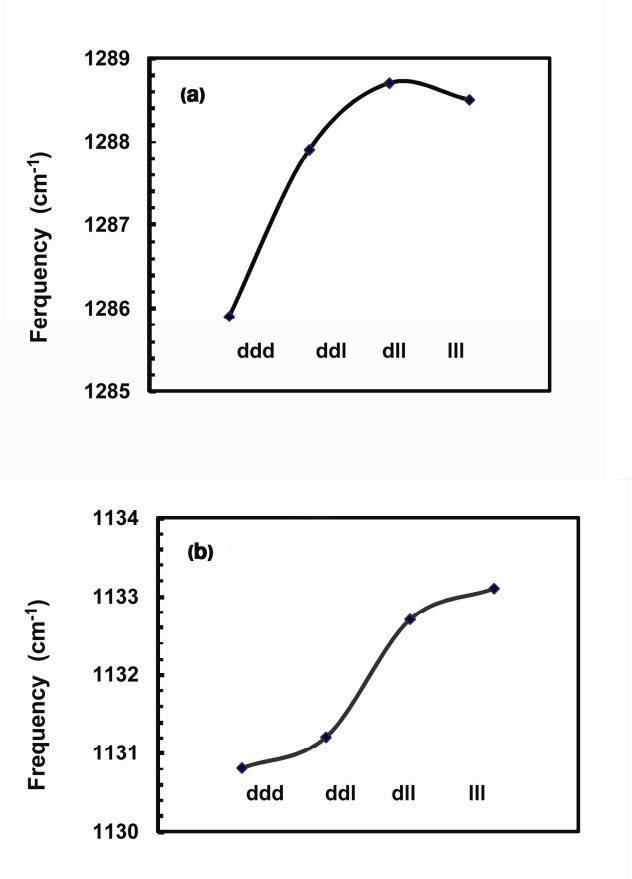


**Fig. 8.** (a) The variation $NH_2$ wagging (b) VCD spectra The variation HCC+HNC bending of the $\nu_{22}$ and $\nu_{29}$ with the conformation change.

## CONCLUSIONS

The calculated relative conformational energies of $[Ni(en)_3]Cl_2$ fell within 0.17 kcal $mol^{-1}$. However, the Δ(λλλ) conformer had the lowest energy and the next highest energy isomer was Δ(δδδ). They occurred in two-thirds of the reported structures presumably because it was the configuration which was easily stabilized by hydrogen bonds. Conversely, the solitary example of the Δ(δδλ) and Δ(δλλ) configurations indicated that it was the higher energy isomers. Furthermore, the large number of strong hydrogen bonds found in the Δ(δδδ) structure supported this assignment. The results for Δ(δδλ) and Δ(δλλ) were a bit ambiguous. This relative rarity warranted placing these configurations as the second highest energy isomer. We thus propose the following

**Table 4.** The g-Tensor Values for $[Ni(en)_3]Cl_2$ and $Ni(en)_3^{2+}$ Using B3LYP/6-31G and B3LYP/6-31G** Levels of Computations

| g-Tensor | $Ni(en)_3^{2+}$ | | | | $Ni(en)_3Cl_2$ | | | | Expt[a] $[Ni(en)_3](NO_3)_2$ |
|---|---|---|---|---|---|---|---|---|---|
| | Δ(λλλ) | Δ(λλδ) | Δ(λδδ) | Δ(δδδ) | Δ(λλλ) | Δ(λλδ) | Δ(λδδ) | Δ(δδδ) | |
| 6-31G | | | | | | | | | |
| $g_x$ | 2.71 | 2.70 | 2.70 | 2.69 | 2.66 | 2.67 | 2.70 | 2.64 | 2.68 |
| $g_y$ | 2.71 | 2.70 | 2.71 | 2.69 | 2.66 | 2.65 | 2.70 | 2.64 | 2.71 |
| $g_z$ | 2.69 | 2.71 | 2.69 | 2.71 | 2.66 | 2.66 | 2.71 | 2.69 | 2.71 |
| 6-31G** | | | | | | | | | |
| $g_x$ | 2.69 | 2.69 | 2.70 | 2.69 | 2.69 | 2.69 | 2.70 | 2.69 | 2.68 |
| $g_y$ | 2.71 | 2.70 | 2.70 | 2.70 | 2.71 | 2.72 | 2.73 | 2.74 | 2.71 |
| $g_z$ | 2.71 | 2.70 | 2.69 | 2.70 | 2.71 | 2.72 | 2.72 | 2.71 | 2.71 |

order of the relative conformational energies of the four unique Δ configuration isomers: Δ(δδδ) < Δ(δδλ) < Δ(δλλ) < Δ(λλλ).

The structural optimization of the complex was done using B3LYP/6-31G. Then, frequencies and EPR g tensor components were calculated using the same approach. Then, g-tensor was diagonalized using Matlab computer program for the $g_x$, $g_y$ and $g_z$ components. The g tensor components $g_x$, $g_y$ and $g_z$ within ±0.04 unit, were the same, reflecting the spherical structure of the complex.

## REFERENCE


[1 ] T.B. Freedman, X. Cao, D.A. Young, L.A. Nafie, J. Phys. Chem. 106 (2002) 3560.

[2 ] J. Autschbach, F.E. Jorge, T. Ziegler, Inorg. Chem. 42 (2003) 2867.

[3 ] G.V. Romanenko, V.L. Varand, N.V. Podberezskaya, D.Y. Naumov, S.A. Gromilov, S.V. Larionov, J. S. Chem. 42 (2001) 1036.

[4 ] E.V. Makotchenko, I.A. Baidina, D.Y. Naumov, J.S. Chem. 47 (2006) 499.

[5 ] W.T. Chen, M.S. Wang, L.Z. Cai, G.C. Guo, J.S. Huang, Aust. J. Chem. 58 (2005) 578.

[6 ] D. Neil, M.J. Riley, C.H.L. Kennard, Acta Cryst. Sec: B 53 (1997) 701.

[7 ] P.V. Bernhardt, M.J. Riley, Aust. J. Chem. 56 (2003) 287.

[8 ] P.V. Bernhardt, L.K. Nathan, Aust. J. Chem. 26 (2007) 329.

[9 ] N. Norani, H. Rahemi, S.F. Tayyari, M.J. Riley, J. Mol. Model. 15 (2009) 25.

[10 ] M.J. Riley, C.R. Wilson, D. Wang, G.R. Hanson, Chem. Phys. 217 (1997) 63.

[11 ] L.S. Prasad, S. Subramanian, J. Chem. Phys. 43 (1987) 88.

[12 ] M.J. Frisch, G.W. Trucks, H.B. Schlegel, G. E. Scuseria, M.A. Robb, J.R. Cheeseman, J. A. Montgomery, Jr., T. Vreven, K.N. Kudin, J.C. Burant, J.M. Millam, S.S. Iyengar, J. Tomasi, V. Barone, B. Mennucci, M. Cossi, G. Scalmani, N. Rega, G.A. Petersson, H. Nakatsuji, M. Hada, M. Ehara, K. Toyota, R. Fukuda, J. Hasegawa, M. Ishida, T. Nakajima, Y. Honda, O. Kitao, H. Nakai, M. Klene, X. Li, J.E. Knox, H.P. Hratchian, J.B. Cross, V. Bakken, C. Adamo, J. Jaramillo, R. Gomperts, R.E. Stratmann, O. Yazyev, A.J. Austin, R. Cammi, C. Pomelli, J.W. Ochterski, P.Y. Ayala, K. Morokuma, G.A. Voth, P. Salvador, J.J. Dannenberg, V.G. Zakrzewski, S. Dapprich, A.D. Daniels, M.C. Strain, O. Farkas, D.K. Malick, A.D. Rabuck, K. Raghavachari, J.B. Foresman, J.V. Ortiz, Q. Cui, A.G. Baboul, S. Clifford, J. Cioslowski, B.B.

Stefanov, G. Liu, A. Liashenko, P. Piskorz, I. Komaromi, R.L. Martin, D.J. Fox, T. Keith, M.A. Al-Laham, C.Y. Peng, A. Nanayakkara, M. Challacombe, P.M.W. Gill, B. Johnson, W. Chen, M.W. Wong, C. Gonzalez, J.A. Pople, Gaussian 03, Revision C.02, Gaussian, Inc., Wallingford CT, 2004.

[13 ] W. Kohn, L.J. Sham, Phys. Rev. A 140 (1965) 1133.

[14 ] S.H. Vosko, L. Wilk, M.C. Nusair, J. Phys. 8 (1980) 12001.

[15 ] A.D. Becke, J. Chem. Phys. 107 (1997) 8554.

[16 ] C. Lee, W. Yang, R.G. Parr, Phys. Rev. B 37 (1988) 785.

[17 ] R.E. Cramer, J.T. Huneke, Inorg. Chem. 14 (1975) 2565.

[18 ] S.F. Pavkovic, D.W. Meek, Inorg. Chem. 4 (1965) 1091.

[19 ] R.E. Cramer, J.T. Huneke, Inorg. Chem. (1978) 369.

[20 ] J.R. Cheeseman, M.J. Frisch, F.J. Devlin, P.J. Stephens, Chem. Phys. Lett. 252 (1996) 211.

[21 ] A.J. Bridgeman, K.M. Jupp, M. Grrloch, Inorg. Chem. 33 (1994) 5424.